Hindawi Publishing Corporation
International Journal of Photoenergy
Volume 2015, Article ID 548984, 10 pages
http://dx.doi.org/10.1155/2015/548984

Research Article

Wet-Chemical Surface Texturing of Sputter-Deposited ZnO:Al Films as Front Electrode for Thin-Film Silicon Solar Cells

Xia Yan,[1,2] Selvaraj Venkataraj,[1] and Armin G. Aberle[1,2,3]

[1]*Solar Energy Research Institute of Singapore, National University of Singapore, 7 Engineering Drive 1, Singapore 117574*
[2]*NUS Graduate School for Integrative Sciences & Engineering (NGS), National University of Singapore, 28 Medical Drive, Singapore 117456*
[3]*Department of Electrical and Computer Engineering, National University of Singapore, 4 Engineering Drive 3, Singapore 117576*

Correspondence should be addressed to Xia Yan; xiayan@u.nus.edu

Received 29 September 2014; Revised 22 January 2015; Accepted 24 January 2015

Academic Editor: Mohammed A. Gondal

Transparent conductive oxides (TCOs) play a major role as the front electrodes of thin-film silicon (Si) solar cells, as they can provide optical scattering and hence improved photon absorption inside the devices. In this paper we report on the surface texturing of aluminium-doped zinc oxide (ZnO:Al or AZO) films for improved light trapping in thin-film Si solar cells. The AZO films are deposited onto soda-lime glass sheets via pulsed DC magnetron sputtering. Several promising AZO texturing methods are investigated using diluted hydrochloric (HCl) and hydrofluoric acid (HF), through a two-step etching process. The developed texturing procedure combines the advantages of the HCl-induced craters and the smaller and jagged—but laterally more uniform—features created by HF etching. In the two-step process, the second etching step further enhances the optical haze, while simultaneously improving the uniformity of the texture features created by the HCl etch. The resulting AZO films show large haze values of above 40%, good scattering into large angles, and a surface angle distribution that is centred at around 30°, which is known from the literature to provide efficient light trapping for thin-film Si solar cells.

1. Introduction

Transparent conductive oxide (TCO) front electrodes are extensively utilised in thin-film silicon (Si) solar cells. Compared to wafer-based Si solar cells, thin-film Si solar cells have a very thin absorber layer (about 200–300 nm for amorphous Si cells and about 1–3 μm for microcrystalline Si cells [1]), which is insufficient for absorbing a large fraction of the incoming solar photons. Therefore the front TCO layer requires a rough surface to scatter incident light into the absorber layer. An efficient light management scheme leads to an elongation of the optical path length in the device and thus a higher chance of photon absorption [1, 2]. As a result, the short-circuit current density (J_{SC}) and the conversion efficiency of the solar cells can be increased.

Commonly used TCO materials include fluorine-doped tin oxide (FTO), tin-doped indium oxide (ITO), and zinc oxide doped with group III impurities (e.g., Al, Ga, and B) [3]. Of these, aluminium-doped zinc oxide (ZnO:Al or AZO) is becoming more favoured as the front electrode for superstrate thin-film solar cell applications, owing to its advantages such as nontoxicity, stability against hydrogen plasma, low cost, and easy postdeposition texturing by wet-chemical etching for light management [4–6].

For magnetron sputtered AZO films, the surface texture is usually obtained through a wet-chemical etching process (resulting in crater-like features) in weak or diluted acids [7], such as hydrochloric acid (HCl), nitric acid (HNO_3), phosphoric acid (H_3PO_4), acetic acid (CH_3COOH), and hydrofluoric acid (HF) [8–14]. Conventional AZO texturing is based on a single etching process using diluted HCl solution. The standard HCl-etched AZO surface commonly has lateral uniformity issues due to an inhomogeneous attack by the HCl acid, regardless of the used HCl concentration [15, 16]. The appearance of small holes is also often observed after HCl etching, which may cause shunting issues for the solar cells [15]. It has been reported that HF etching of AZO is more uniform than HCl etching [16]. As a weak acid,

HF tends to only slightly dissociate in water. Undissociated HF molecules are relatively small compared to the water hydronium cluster (e.g., H_3O^+) and thus can penetrate deep into grain boundaries before the start of the chemical reaction [12]. Thus HF is able to create a higher density of attack points than HCl, which contributes to more homogenously etched textures [17].

Therefore, a two-step texturing procedure based on etching in HCl and HF is tested in this study. The idea behind the two-step process is to improve the lateral uniformity of the surface texture and also to further enhance the light scattering via HF etching. In order to achieve a homogeneously textured surface with enhanced light scattering capabilities, in this work we systemically investigate (i) single-step HCl or HF etching as the reference, (ii) two-step etching procedure using HF and then HCl acid, and (iii) two-step etching procedure using HCl and then HF acid for the surface texturisation of AZO films. For these experiments, pulsed DC sputtered AZO films with high transmission ($T_{vis} > 85\%$) in the visible wavelength range and low resistivity (~8×10^{-4} Ωcm) are used.

2. Experimental Details

2.1. Deposition of AZO Samples. AZO films were deposited onto planar A3 size (30 cm × 40 cm) soda-lime glass sheets by an inline multichamber magnetron sputter machine (Model Line 540 from FHR Anlagenbau GmbH) using a pulsed DC power supply [18]. Dual cylindrical $ZnO : Al_2O_3$ (98 : 2 wt%) rotatable ceramic targets were used to deposit the AZO films. The applied power for each cathode was kept constant at 2 kW. During deposition, the substrate heater temperature was kept constant at 350°C (the corresponding substrate temperature was maintained at about 190°C). The chamber pressure was maintained at 3×10^{-3} mbar by introducing pure argon and oxygen-diluted argon (1% O_2 and 99% Ar) as processing gases via mass flow controllers (MFCs) at constant flow rates of 155 and 50 sccm, respectively.

The deposition was carried out in dynamic mode (i.e., moving substrate). During deposition, the glass sheet was vertically attached (i.e., portrait format) on a moving carrier and allowed to oscillate 18 times in front of the AZO sputter cathodes, at a moving speed of 10 mm/s. This multiple-pass deposition potentially reduces the formation of pinholes and thus benefits the subsequent etching process [19]. The rotating speed of the targets was kept constant at 10 rpm for all depositions. After deposition, the AZO-coated glass sheets were cut into 12 square pieces (each 10 cm × 10 cm) for the wet-chemical surface texturing experiments.

All the acids used for the AZO texturisation experiments were diluted into aqueous solutions and are represented via their volume fraction (vol%). Although diluted HF solutions can still attack the glass substrates, the reaction proceeds at a very slow speed and barely affects the glass flatness [16]. Hence, the effect of glass etching was neglected in this study.

2.2. Characterisation. The optical properties of AZO films were characterised with a double-beam UV/Vis/NIR spectrophotometer featuring a 150 mm diameter integrating sphere (PerkinElmer, LAMBDA 950), which records the reflectance and transmittance spectra (diffuse and total) from 300 to 1200 nm before and after texturing the AZO films. The diffuse transmittance was measured by opening the reflectance port at the rear of the integrating sphere and thereby letting the specular light escape from the integrating sphere. The haze value was calculated via

$$\text{Haze}\,(\%) = \frac{T_{\text{diff}}}{T_{\text{total}}} \times 100, \tag{1}$$

where Haze, T_{diff}, and T_{total} are the transmission haze, the diffuse transmittance, and the total transmittance, respectively. In addition to the spectrophotometer measurements, visible transmission and haze values (in the 350–700 nm range) of the textured AZO films were also recorded with a haze meter (BYK-Gardner, haze-gard plus) to quantitatively evaluate the optical performance. The electrical performance of the AZO films was represented by the sheet resistance value, which was measured with the four-point probe method (Napson, CRESBOX).

The AZO film thicknesses were obtained by curve fitting of the measured spectral transmittances, using the commercial optical simulation software CODE [20]. Three dielectric models were used to model the optical properties of the AZO films: the O'Leary-Johnson-Lim (OJL) model, the extended Drude (EDR) model, and Kim's oscillator model. Details about the fitting method can be found in [20, 21]. The surface morphology resulting from texturing the AZO films was analysed by scanning electron microscopy (SEM; Carl Zeiss, Auriga-39-35) and atomic force microscopy (AFM; Veeco, NanoScope D3100). The AFM images were taken in the central region of each sample, using the tapping mode at a scan rate of 0.5 Hz. The image scan size was set as 10 μm × 10 μm for all samples.

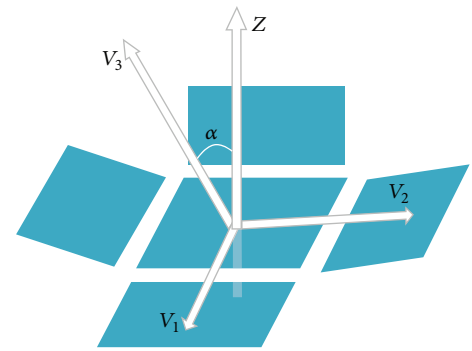

Figure 1: Definition of the vectors and surface inclination angle used in the MATLAB image processing method.

2.3. Analysis of Surface Inclination Angle. Statistical analysis of the surface inclination angle of textured AZO samples was carried out based on the AFM measurements and a MATLAB image processing programme [22–24]. Each AFM image consists of 512 × 512 data points, and each data pixel contains the local height information. Consider the pixel in the centre (as illustrated in Figure 1), vector one ($\mathbf{V_1}$ vertical tangent vector), and vector two ($\mathbf{V_2}$ horizontal tangent

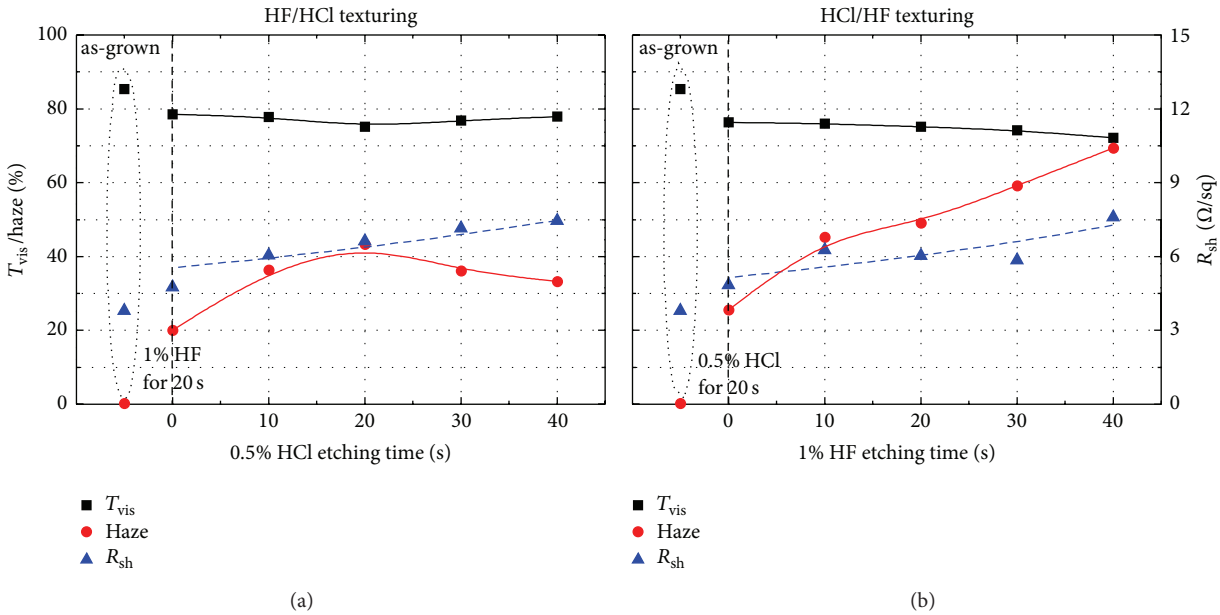

FIGURE 2: Variation of visible transmission (T_{vis}), haze value (measured with the haze meter), and sheet resistance (R_{sh}) of two-step textured AZO films as a function of the duration of the second etching step, for (a) HF/HCl etching and (b) HCl/HF etching.

vector) connect the central pixel with its neighbouring pixels, which describes the orientation of the planar surface of the central pixel. Vector three ($\mathbf{V_3}$) is perpendicular to the studied surface, thus calculated by the cross product of $\mathbf{V_1}$ and $\mathbf{V_2}$ via

$$\mathbf{V_3} = \mathbf{V_1} \times \mathbf{V_2}. \quad (2)$$

Based on these vectors, the inclination angle (α) is calculated as the angle between the normal vector ($\mathbf{V_3}$) of the plane in respect to the z-axis (the axis perpendicular to the mean surface level, represented by vector $\mathbf{Z}$). The angle distributions of the surface textures are then statistically analysed and quantified into a histogram with 5-degree increments. The literature suggests that a surface angle distribution centred at about 30° provides effective light trapping for thin-film Si solar cell applications [24, 25].

3. Results and Discussion

For comparison, two sets of etching experiments were carried out in this work. In the first set, AZO samples were textured using 1% HF for 20 s (step 1) and then further etched using 0.5% HCl (step 2) from 0 to 40 s (noted as HF/HCl etching). For the second set, AZO films were textured using 0.5% HCl for 20 s (step 1) and then further etched using 1% HF (step 2) from 0 to 40 s (noted as HCl/HF etching).

These as-grown AZO films show a low sheet resistance of 3.8 Ω/□ with a thickness of around 1.8 μm. After 20 s of HF or HCl etching (step 1), both the sheet resistance had increased to around 4.8 Ω/□. After the second etching step, the corresponding sheet resistance had further increased to 7.3 and 7.5 Ω/□ (see Figures 2(a) and 2(b)), due to the reduced film thickness. Using the thickness value obtained from CODE (as described in Section 2.2), it follows that the AZO etching rates in 0.5% HCl and 1% HF are approximately the same (15–20 nm/s). This explains why the etching sequence seems to have little effect on the change of the sheet resistance value.

In contrast to the electrical performance, the optical properties are quite sensitive to the etching sequence. The values measured with the haze meter (see Figure 2) well agree with the spectral variations measured with the spectrophotometer (see Figure 3). Before texturing, these as-grown AZO films show a high visible transmission value fluctuating around 85% but virtually no scattering capabilities with a haze value of approximately 1%. With respect to HF/HCl etching, the first step HF-etched AZO film yields a haze value of 14% at 600 nm wavelength. A maximum haze value of 31% is obtained after the second step HCl etching for 20 s. Further etching above 30 s gradually deteriorates the haze value by up to 10% (see Figure 3(b)). A similar trend is observed in the optical transmittance value (see Figure 3(a)), which reduces from around 85% (as-grown) to a minimum value of 70% at 600 nm when the second etching step (HCl) lasted 20 s and then slightly rebounces to 73% while further etching to 40 s.

A different scenario is observed for the reversed two-step etching sequence (HCl/HF). In this case the spectral profiles show that, with increasing duration of the second etching step (HF), the AZO films gradually become more scattering. The HCl-etched AZO film shows a haze value of 22% at 600 nm wavelength, which further increases to 54% when the second step HF etching time increases to 40 s (see Figure 3(d)). The film transmission into air slightly decreases from 72% to 67% at 600 nm wavelength through the second step HF etching from 0 to 40 s (see Figure 3(c)). At the same time, the near-infrared (NIR) transmission starts to improve from ~900 nm wavelength due to reduced free carrier absorption for thinner films. For both two-step etching processes (HF/HCl and

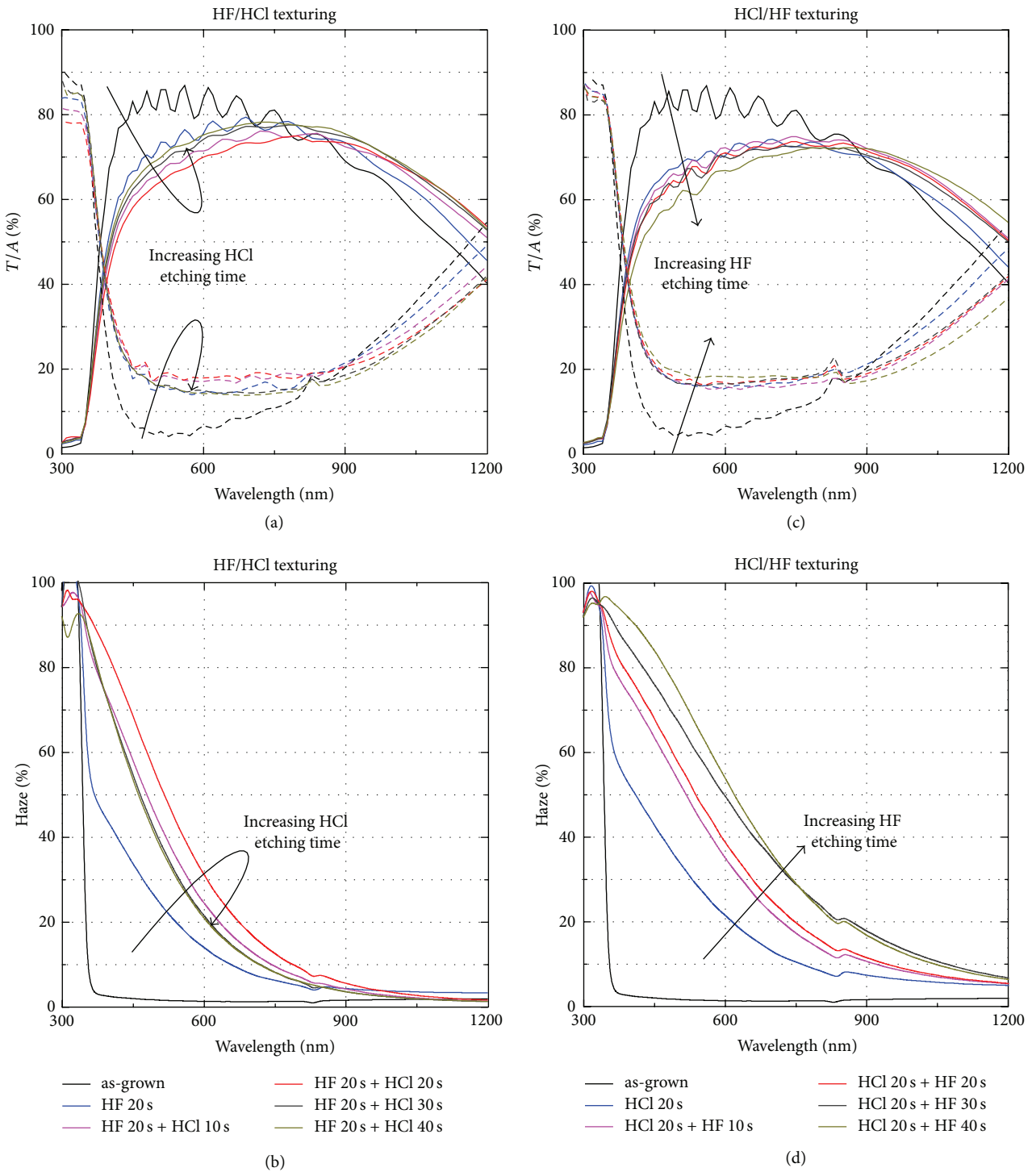

Figure 3: ((a) and (c)) Optical transmittance (solid line) and absorbance (dash line), and ((b) and (d)) haze as a function of wavelength for two-step textured AZO by (left) HF/HCl etching and (right) HCl/HF etching. Arrows indicate the trends for increasing duration of the second etching step.

HCl/HF), regardless of the duration of the second etching step, the transmission into air is only weakly affected and, at around 600 nm wavelength, generally lies in the narrow range of 70 ± 3%; see Figures 3(a) and 3(c). It is also important to note that the actual value of the transmission into Si should be much higher than the value measured into air owing to a much high refractive index of the Si material.

The SEM micrographs in Figures 4(a)–4(e) and 4(f)–4(j) show the evolution of the AZO surface morphology during the second etching step, for the two investigated etching

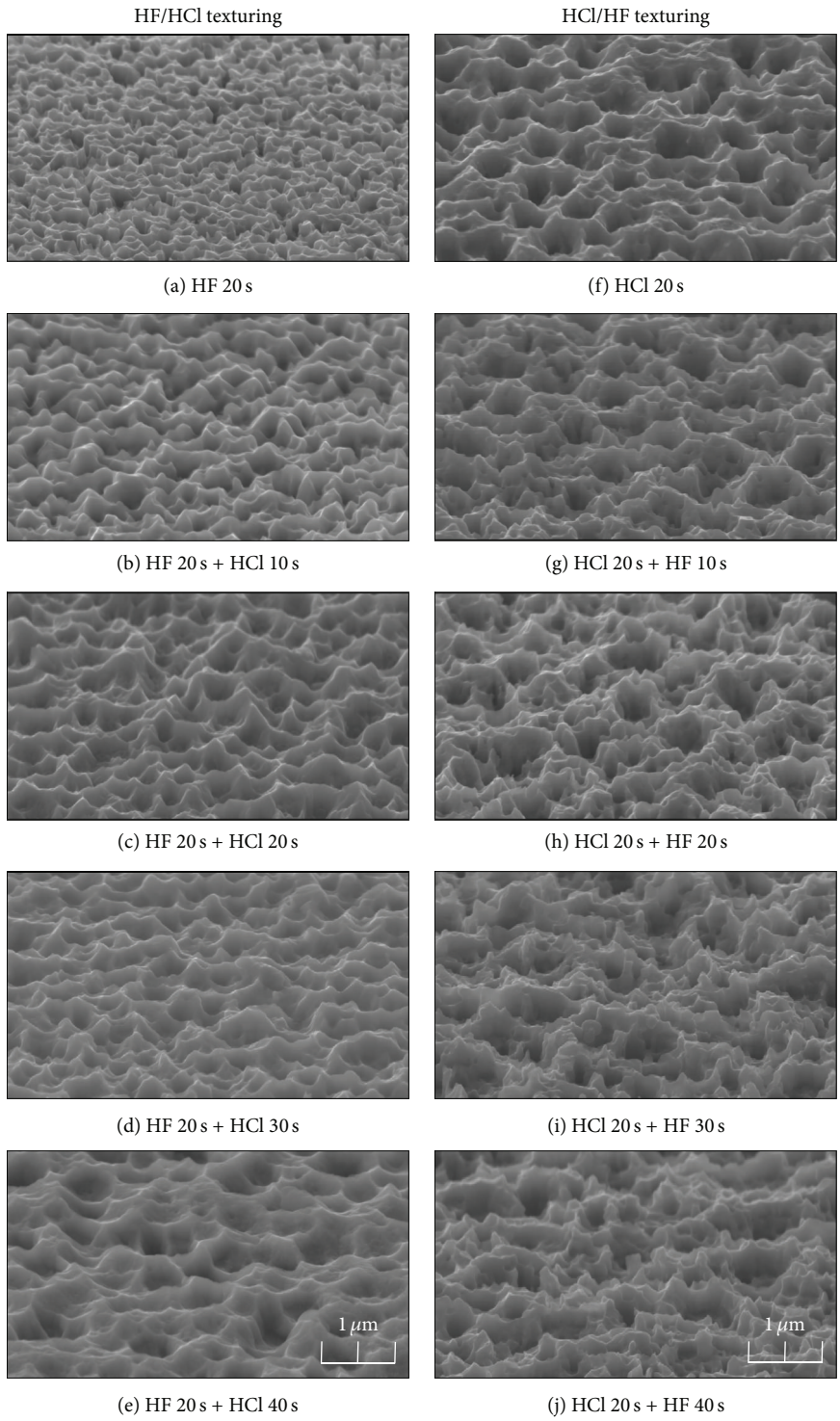

Figure 4: SEM micrographs of AZO films textured with the two-step sequences (left = HF/HCl, right = HCl/HF). (Left) 1% HF etching for 20 s and then 0.5% HCl etching for (a) 0 s, (b) 10 s, (c) 20 s, (d) 30 s, and (e) 40 s. (Right) 0.5% HCl etching for 20 s and then 1% HF etching for (f) 0 s, (g) 10 s, (h) 20 s, (i) 30 s, and (j) 40 s. During the measurements the samples were tilted by 60° and the images were recorded with a magnification of 25000.

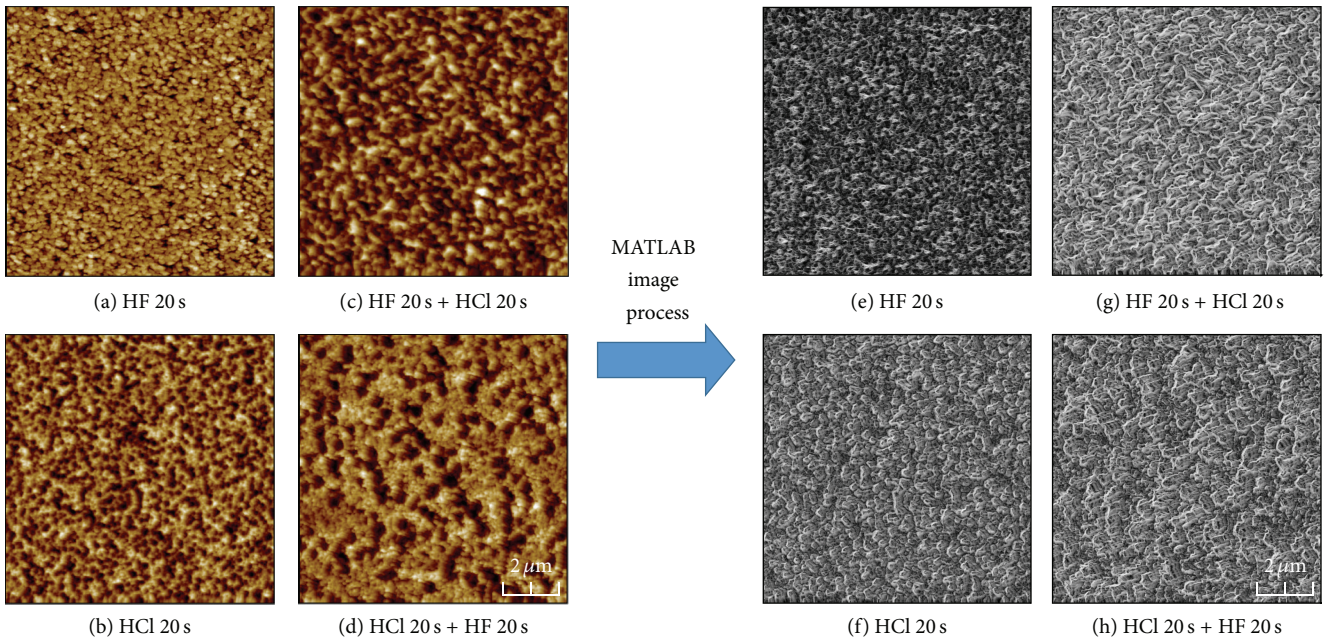

Figure 5: Measured AFM 2D images and MATLAB processed images of AZO films textured with ((a) and (e)) a single-step etch of HF for 20 s, ((b) and (f)) a single-step etch of HCl for 20 s, ((c) and (g)) a two-step etch of HF for 20 s and HCl for 20 s, and ((d) and (h)) a two-step etch of HCl for 20 s and HF for 20 s.

sequences. With regard to the HF/HCl sequence, the HCl etching step gradually removes a certain amount of HF-induced features while introducing HCl-induced craters; see Figures 4(b) to 4(e). As a result, the corresponding haze value initially increases, then reaches a maximum, and then decreases again for etching times of more than 20 s. For 40 s of HCl etching (see Figure 4(e)) a surface morphology is obtained which looks similar to that solely etched by HCl acid (see Figure 4(f)). In this case, further etching would overetch the AZO film by complete removal of these first step HF-induced features.

For the HCl/HF sequence the SEM micrographs show (see Figures 4(f) to 4(j)) that lots of small jagged HF-induced features gradually evolve and superimposedly grow on top of the HCl-etched craters. Even after relatively long etching in HF (e.g., 40 s, which is twice as long as the duration of the first etching step in HCl), the dominant surface features are still these HCl-induced craters (see Figure 4(j)). Therefore, for strong scattering, it is preferred to first use HCl to texture the AZO film, followed by etching in diluted HF to optimise the features and thus enhance the haze value. Around 20 or 30 s of HF etching is enough to achieve a good scattering, and further etching seems not to improve much anymore. From the SEM observation, it is also confirmed that the lateral uniformity of the surface textures benefits from the second step HF etching.

Figure 5 compares AFM 2D images (see Figures 5(a)–5(d)) of AZO films textured with different etching procedures and the corresponding processed images (see Figures 5(e)–5(h)). In order to better understand the light scattering capabilities of these textured films, as described in Section 2.3, the measured AFM images were processed using a MATLAB programme to determine information on the surface height and inclination angle of the texture features.

The feature height and angle distributions of the textured surface are then calculated from AFM and MATLAB simulations. Figures 6(a) and 6(c) show the height histograms of the AZO films textured with the two sets of two-step texturing methods. The HF-induced texture has a very narrow height distribution, while the additional HCl etching broadens the height distribution for the HF/HCl etching sequence. In contrast, the second step HF etching slightly widens and shifts the height distribution of HCl-etched film, for the HCl/HF etching. From the literature it is well known that a broad surface height distribution is beneficial for light trapping in thin-film Si solar cells, for a wide range of wavelengths [26]. In this case, two-step textured AZO shows a better height distribution than either HCl or HF solely etched film.

Figures 6(b) and 6(d) compare the distribution of the surface inclination angles of these two-step textured AZO films. Texturing in HF for 20 s results in an angle distribution that peaks at about 20°; see Figure 6(b). Subsequent etching in HCl for 10 to 40 s shifts the peak by 15–20° to the right and simultaneously widens the angle distribution. In contrast, first texturing in HCl yields a narrow distribution with a peak maximum at 30°. Subsequent etching in HF for 10 to 40 s causes only slight changes to both the peak position (<5°) and the width of the distribution curve; see Figure 6(d).

In addition to the surface height and angle, the feature size also plays an essential role in the light scattering process. One of the most commonly used methods to describe the surface feature of textured AZO films is to use the power spectral density (PSD) function [27, 28]. The two-dimensional (2D) isotropic PSD function is derived by the fast Fourier

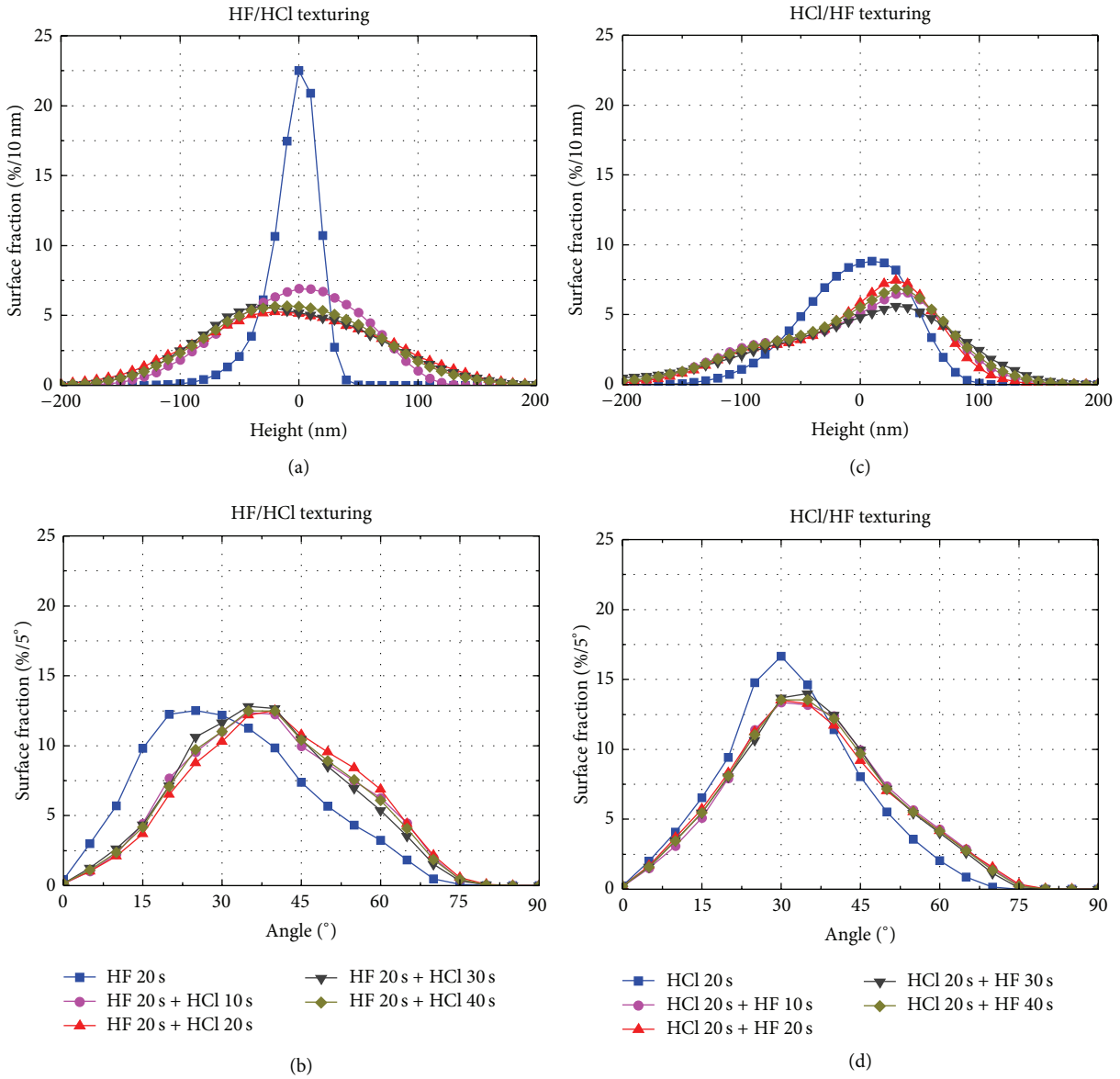

FIGURE 6: ((a) and (c)) Surface height and ((b) and (d)) angle distribution histograms derived from AFM measurements for two-step textured AZO films using (left) 1% HF etching for 20 s and then 0.5% HCl etching from 0 to 40 s, (right) 0.5% HCl etching for 20 s, and then 1% HF etching from 0 to 40 s.

transform (FFT) of the AFM scans of the surface-textured AZO films [27, 29].

Figures 7(a) and 7(c) compare the distribution of the PSD function of the two-step textured AZO films. The inverse of the x-scale (spatial frequency) represents the lateral feature sizes of the surface texture; that is, a low spatial frequency represents a large lateral features size. A higher PSD intensity indicates that the corresponding lateral feature size is more dominant in the textured surface. In order to effectively scatter the incoming light, the lateral feature size of the surface texture should be comparable to the effective wavelength ($\lambda_{\text{eff}} = \lambda_{\text{air}}/n_{\text{AZO}}$) [30], that is, around 300 to 600 nm. It is clearly observed that the lateral size of the HCl-induced texture is much larger than that of the HF-induced texture, and the second step etching can further expand the lateral size of the texture features.

The PSD function can also provide an exact value to represent the surface morphology of the textured films, such as the root-mean-square (RMS) roughness (σ_{RMS}) and the autocorrelation length (τ_{cl}), as shown in Figures 7(b) and 7(d). The RMS roughness represents how rough the textured surface is, and the autocorrelation length corresponds to the average lateral size of the randomly textured surface [31]. The two-step textured AZO films prepared by HF and then HCl etching tends to have a small lateral size of around 150 nm, attributed to the small HF-induced textures. In contrast, the AZO films textured by HCl etching for 20 s and then HF etching for 30 or 40 s show a good average lateral feature

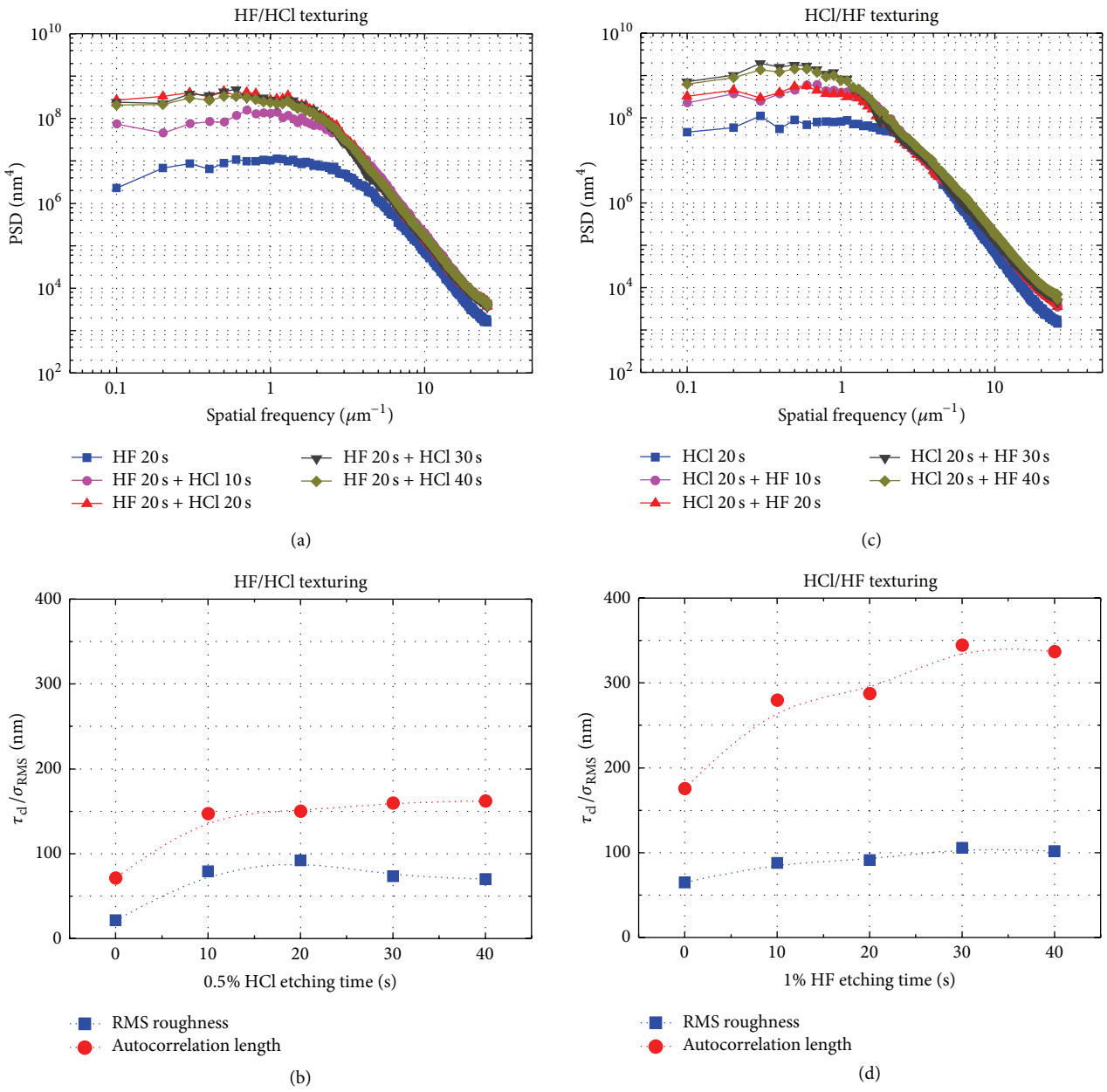

FIGURE 7: ((a) and (c)) Power spectral density (PSD) function and ((b) and (d)) corresponding autocorrelation length and RMS roughness derived from AFM measurements for two-step textured AZO films using (left) 1% HF etching for 20 s and then 0.5% HCl etching from 0 to 40 s, (right) 0.5% HCl etching for 20 s, and then 1% HF etching from 0 to 40 s.

size of around 340 nm, comparable to the effective scattering feature sizes. In addition, the RMS roughness of such two-step textured AZO films is around 100 nm, which is in the acceptable range for solar cell fabrication (note that excessive surface roughness will cause shunting issues in solar cell diodes).

Angular resolved scattering (ARS) defines the distribution of diffuse scattered light between 0° and 90°. The light intensity at an angle of 0° represents the specularly transmitted light (i.e., the nonscattered light). In this work, the ARS of the transmitted light for the textured AZO films was simulated based on the phase model by using experimental AFM images and the refractive indices of the two media (AZO/air interface) [32]. The typical solar wavelength of 600 nm is used for the calculation. The calculated ARS results are normalised so that the total integrated transmission is equal to unity. Figure 8 shows the simulated ARS of the two-step textured AZO films. The zig-like profile line is due to the finite resolution of AFM scan [33].

A good correlation is observed between the calculated ARS results of Figure 8 and the optical haze measurements of Figure 3. From these experiments, as stated above, the second etching step greatly enhances optical scattering (represented by a high haze value and ARS intensity) for both texturing

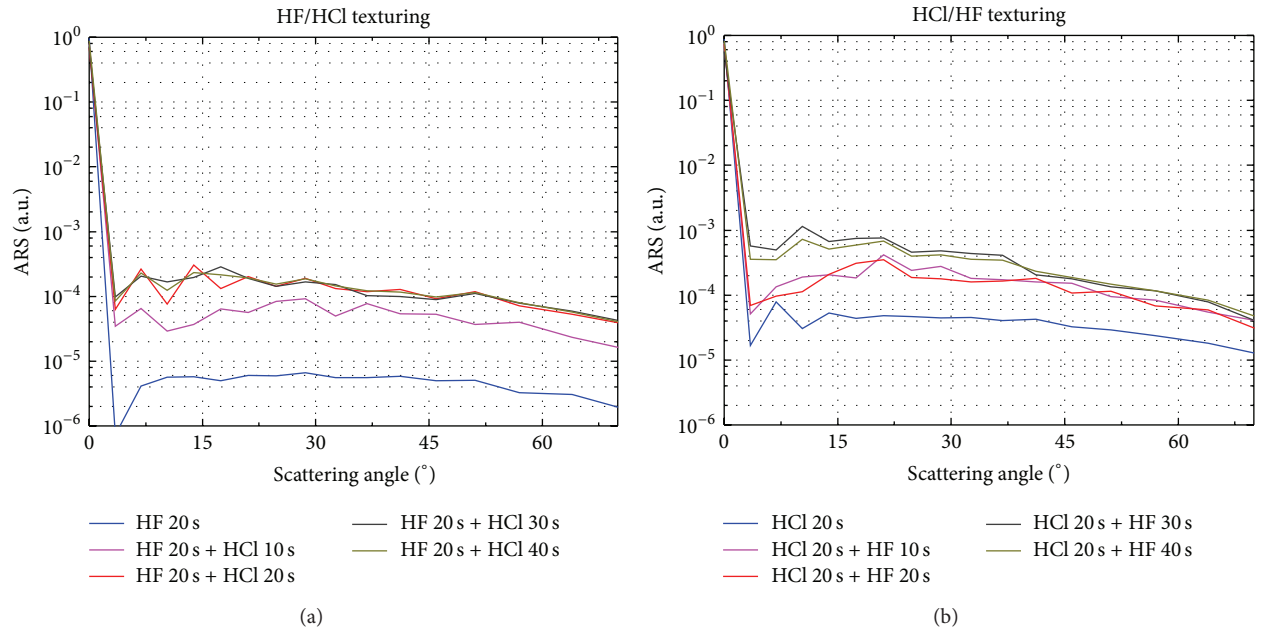

Figure 8: Angular resolved scattering (ARS) of transmission into air derived from AFM measurements for two-step textured AZO films using (a) 1% HF etching for 20 s and then 0.5% HCl etching from 0 to 40 s and (b) 0.5% HCl etching for 20 s and then 1% HF etching from 0 to 40 s.

procedures. These textured films also show good ARS intensity at large scattering angles. The ARS results indicate that the two-step etching procedure that starts with HCl is more user-friendly, as a wide range of second-step etching times gives maximum scattering properties.

4. Conclusions

In this paper, wet-chemical texturing of pulsed DC sputtered AZO films was investigated using several etching processes: (i) single-step etching in HCl or HF acid as the reference, (ii) two-step etching in HF acid and then HCl acid, and (iii) two-step etching in HCl acid and then HF acid. Although the texturing increases the sheet resistance value of the AZO films due to reduced film thickness, there is no much difference between these different etching methods.

Compared to standard HCl-etched AZO, it is advantageous to use two-step texturing to modify the surface morphology for better optical performance. The two-step textured AZO films, initially textured in HCl and then in HF (e.g., 20 or 30 s), which slightly modified the texture features, have stronger light scattering capabilities (haze values of above 40% and good ARS intensity at large scattering angles), while maintaining similar optical transmission (~70% transmission into air at 600 nm wavelength) and a good surface angle distribution (centred at around 30°). The two-step textured films also show better lateral texture uniformity than the standard HCl-etched films, owing to the HF etching step. Thus, it is expected that the two-step texturing method (etching in HCl acid and then HF acid) produces the best performing AZO films for thin-film Si solar cell applications.

Conflict of Interests

The authors declare that there is no conflict of interests regarding the publication of this paper.

Acknowledgments

The Solar Energy Research Institute of Singapore (SERIS) is sponsored by the National University of Singapore (NUS) and Singapore's National Research Foundation (NRF) through the Singapore Economic Development Board (EDB). This research was supported by the NRF, Prime Minister's Office, Singapore, under its Clean Energy Research Programme (CERP, Award no. NRF2011EWT-CERP001-019). Xia Yan acknowledges a Ph.D. scholarship jointly funded by SERIS and the NUS Graduate School for Integrative Sciences and Engineering (NGS).

References

[1] J. Müller, B. Rech, J. Springer, and M. Vanecek, "TCO and light trapping in silicon thin film solar cells," *Solar Energy*, vol. 77, no. 6, pp. 917–930, 2004.

[2] J. Hüpkes, S. E. Pust, W. Böttler et al., "Light scattering and trapping in different thin film photovoltaic device," in *Proceedings of the 24th European Photovoltaic Solar Energy Conference and Exhibition*, pp. 2766–2769, Hamburg, Germany, September 2009.

[3] L. Castañeda, "Present status of the development and application of transparent conductors oxide thin solid films," *Materials Sciences and Applications*, vol. 2, no. 9, pp. 1233–1242, 2011.

[4] J. Müller, G. Schöpe, O. Kluth et al., "Upscaling of texture-etched zinc oxide substrates for silicon thin film solar cells," *Thin Solid Films*, vol. 392, no. 2, pp. 327–333, 2001.

[5] J. Hu and R. G. Gordon, "Textured aluminum-doped zinc oxide thin films from atmospheric pressure chemical-vapor deposition," *Journal of Applied Physics*, vol. 71, no. 2, pp. 880–890, 1992.

[6] R. Groenen, J. L. Linden, H. R. M. van Lierop, D. C. Schram, A. D. Kuypers, and M. C. M. van de Sanden, "Expanding thermal plasma for deposition of surface textured ZnO:Al with focus on thin film solar cell applications," *Applied Surface Science*, vol. 173, no. 1-2, pp. 40–43, 2001.

[7] Y. Nasuno, M. Kondo, and A. Matsuda, in *Proceedings of the Conference Record of the 28th IEEE Photovoltaic Specialists Conference*, pp. 142–145, 2000.

[8] W.-L. Lu, K.-C. Huang, C.-H. Yeh, C.-I. Hung, and M.-P. Houng, "Investigation of textured Al-doped ZnO thin films using chemical wet-etching methods," *Materials Chemistry and Physics*, vol. 127, no. 1-2, pp. 358–363, 2011.

[9] O. Kluth, B. Rech, L. Houben et al., "Texture etched ZnO:Al coated glass substrates for silicon based thin film solar cells," *Thin Solid Films*, vol. 351, no. 1-2, pp. 247–253, 1999.

[10] E. Bunte, H. Zhu, J. Hüpkes, and J. Owen, "Novel texturing method for sputtered zinc oxide films prepared at high deposition rate from ceramic tube targets," *EPJ Photovoltaics*, vol. 2, Article ID 20602, 2011.

[11] H. Zhu, J. Hüpkes, E. Bunte, J. Owen, and S. M. Huang, "Novel etching method on high rate ZnO:Al thin films reactively sputtered from dual tube metallic targets for silicon-based solar cells," *Solar Energy Materials and Solar Cells*, vol. 95, no. 3, pp. 964–968, 2011.

[12] J. I. Owen, J. Hüpkes, H. Zhu, and E. Bunte, "Controlling the surface texture of sputtered ZnO: Al using different acidic single- or multi-step etches for applications in thin-film silicon solar cells," in *Photovoltaics International*, pp. 52–57, SNEC Exclusive, 10th edition, 2011.

[13] W. T. Yen, Y. C. Lin, and J. H. Ke, "Surface textured ZnO:Al thin films by pulsed DC magnetron sputtering for thin film solar cells applications," *Applied Surface Science*, vol. 257, no. 3, pp. 960–968, 2010.

[14] X.-J. Wang, H. Wang, W.-L. Zhou, G.-X. Li, and J. Yu, "Preparation and character of textured ZnO:Al thin films deposited on flexible substrates by RF magnetron sputtering," *Materials Letters*, vol. 65, no. 13, pp. 2039–2042, 2011.

[15] S. Fernández, O. de Abril, F. B. Naranjo, and J. J. Gandía, "High quality textured ZnO:Al surfaces obtained by a two-step wet-chemical etching method for applications in thin film silicon solar cells," *Solar Energy Materials and Solar Cells*, vol. 95, no. 8, pp. 2281–2286, 2011.

[16] J. I. Owen, J. Hüpkes, H. Zhu, E. Bunte, and S. E. Pust, "Novel etch process to tune crater size on magnetron sputtered ZnO:Al," *Physica Status Solidi A*, vol. 208, no. 1, pp. 109–113, 2011.

[17] K. W. Kolasinski, "The composition of fluoride solutions," *Journal of the Electrochemical Society*, vol. 152, no. 9, pp. J99–J104, 2005.

[18] X. Yan, S. Venkataraj, and A. G. Aberle, "Modified surface texturing of aluminium-doped zinc oxide (AZO) transparent conductive oxides for thin-film silicon solar cells," *Energy Procedia*, vol. 33, pp. 157–165, 2013.

[19] V. Sittinger, F. Ruske, W. Werner et al., "ZnO:Al films deposited by in-line reactive AC magnetron sputtering for a-Si:H thin film solar cells," *Thin Solid Films*, vol. 496, no. 1, pp. 16–25, 2006.

[20] W. Theiss, *Hard- and Software for Optical Spectroscopy*, 2002, http://www.mtheiss.com/.

[21] Z. Qiao, C. Agashe, and D. Mergel, "Dielectric modeling of transmittance spectra of thin ZnO:Al films," *Thin Solid Films*, vol. 496, no. 2, pp. 520–525, 2006.

[22] H. Stiebig, M. Schulte, C. Zahren, C. Haase, B. Rech, and P. Lechner, "Light trapping in thin-film silicon solar cells by nano-textured interfaces," in *Photonics for Solar Energy Systems*, vol. 6197 of *Proceedings of the SPIE*, Strasbourg, France, April 2006.

[23] S. Venkataraj, J. Wang, P. Vayalakkara, and A. G. Aberle, "Light scattering enhancement by double scattering technique for multijunction thin-film silicon solar cells," *IEEE Journal of Photovoltaics*, vol. 3, no. 2, pp. 605–612, 2013.

[24] J. Wang, S. Venkataraj, C. Battaglia, P. Vayalakkara, and A. G. Aberle, "Analysis of optical and morphological properties of aluminium induced texture glass superstrates," *Japanese Journal of Applied Physics*, vol. 51, no. 10, Article ID 10NB08, 2012.

[25] M. Berginski, J. Hüpkes, M. Schulte et al., "The effect of front ZnO:Al surface texture and optical transparency on efficient light trapping in silicon thin-film solar cells," *Journal of Applied Physics*, vol. 101, no. 7, Article ID 074903, 2007.

[26] Y. Wang, X. Zhang, L. Bai, Q. Huang, C. Wei, and Y. Zhao, "Effective light trapping in thin film silicon solar cells from textured Al doped ZnO substrates with broad surface feature distributions," *Applied Physics Letters*, vol. 100, no. 26, Article ID 263508, 2012.

[27] R. H. Franken, R. L. Stolk, H. Li, C. H. M. van der Werf, J. K. Rath, and R. E. I. Schropp, "Understanding light trapping by light scattering textured back electrodes in thin film n-i-p-type silicon solar cells," *Journal of Applied Physics*, vol. 102, no. 1, Article ID 014503, 2007.

[28] J. Escarré, K. Söderström, C. Battaglia, F.-J. Haug, and C. Ballif, "High fidelity transfer of nanometric random textures by UV embossing for thin film solar cells applications," *Solar Energy Materials and Solar Cells*, vol. 95, no. 3, pp. 881–886, 2011.

[29] B. Liu, L. Bai, X. Zhang et al., "Light management in hydrogenated amorphous silicon germanium solar cells," *Solar Energy Materials and Solar Cells*, vol. 128, pp. 1–10, 2014.

[30] R. Dewan, M. Marinkovic, R. Noriega, S. Phadke, A. Salleo, and D. Knipp, "Light trapping in thin-film silicon solar cells with submicron surface texture," *Optics Express*, vol. 17, no. 25, pp. 23058–23065, 2009.

[31] J. M. Bennett and L. Mattsson, *Introduction to Surface Roughness and Scattering*, Optical Society of America, 1989.

[32] D. Dominé, F.-J. Haug, C. Battaglia, and C. Ballif, "Modeling of light scattering from micro- and nanotextured surfaces," *Journal of Applied Physics*, vol. 107, Article ID 044504, 2010.

[33] M. Schulte, K. Bittkau, K. Jäger, M. Ermes, M. Zeman, and B. E. Pieters, "Angular resolved scattering by a nano-textured ZnO/silicon interface," *Applied Physics Letters*, vol. 99, no. 11, Article ID 111107, 2011.